Global Sea Surface Temperatures and Associated Long-Range Predictability of the Northern Hemisphere Circulation and Local Climatological Variables

Ernest C. Kung[1], Jonq-Gong Chern[2] and Diane E. Smith[3]

ABSTRACT

Principal components of the monthly global analyses of sea surface temperatures (SSTs) for the period of 1955-1993 are utilized to study the large-scale modes of SST variations in association with the variability and predictability of atmospheric circulation. The first and second components of the SST field well describe the occurrence of El Niño episodes in terms of the El Niño index (ENI), which is defined as the weighted mean of the coefficients of the first and second components. The coupling modes of the ocean-atmosphere system are examined by correlation analysis of the principal components of SSTs and those of upper-air circulation fields. The El Niño mode strongly influences the winter tropospheric circulation in the middle latitudes for up to three leading seasons. A possible utilization of the ENI in the seasonal-range projection of atmospheric circulation is indicated by the cross-correlation between the preceding ENIs and the following tropospheric circulation for both winter and summer circulation. For the dominance of the El Niño type anomaly fields in the past decade, the principal components of SSTs during the period of July 1991 to December 1993 are also presented.

The feasibility of local long-range forecasting is explored in association with SST anomalies for Taiwan Mei-Yu and for monthly temperature and precipitation over the United States. For Taiwan Mei-Yu, in utilizing the useful complimentary characteristics of the winter El Niño mode and residual components of SST anomalies, the possibility of regional forecasting is examined. For the U.S. climatological stations, teleconnections between principal components of SSTs and monthly temperature and precipitation indicate the usefulness of the former as predictors.

(Key words: El Niño, Mei-Yu, Tele connection)

---

[1] Department of Soil and Atmospheric Sciences, University of Missouri-Columbia, Columbia, Missouri 65211, U.S.A

[2] Central Weather Bureau, Kung Yuan Road 64, Taipei, Taiwan, R.O.C.

[3] National Weather Service/NOAA, Kansas City, Missouri, USA
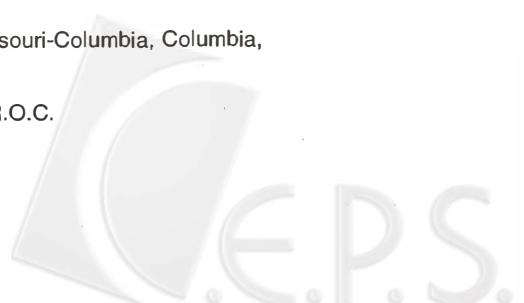
1. INTRODUCTION

In the evolution of large-scale circulation patterns, ocean-atmosphere heat transfer acts as a major boundary forcing the atmosphere. Since the characteristic time-scale of the ocean is much longer than that of the atmosphere, the sea surface temperatures (SSTs) are an ideal predictor in the long-range forecasting of the atmosphere. The importance of SST anomaly fields in forecasting atmospheric circulation is underscored by previous numerical experiments by these authors. It was demonstrated in Kung *et al.* (1990, 1992) that by updating the model with observed SST anomalies during the period of numerical integration, a conventional general circulation model was able to extend the predictability of operational deterministic forecasting to a period of 1 to 1.5 months.

Many climatological studies have been conducted on the interactive features of the ocean and atmosphere. These studies form the basis for empirical long-range forecasting in the range of one month to several seasons. The principal components, which are also referred to as empirical orthogonal functions or eigenvectors, have been used by many researchers in analyzing large-scale variations in ocean and atmospheric circulation (e.g., Kutzbach, 1967; Kidson, 1975; Weare *et al.*, 1976; Heddinghaus and Kung, 1980; Trenberth and Paolino, 1981; Kawamura, 1984; Park and Kung, 1988). Such analyses reduces a large number of variables to a manageable set of components, while still retaining the maximum variance of the original variables. In the analysis of highly correlated meteorological fields, a limited number of principal components may, therefore, effectively represent the basic modes of the variations. Since the empirical orthogonal functions have no predetermined forms, depending only on the interrelationship within the dataset of analysis, they are particularly suitable in the investigation of anomalous fields of the general circulation, for which no known analytical form exists because of complex boundary conditions and various scales of nonlinear interactions.

In a preceding study (Kung and Chern, 1994), large-scale modes of variations of SSTs have been examined with major principal components utilizing monthly mean fields of SSTs during the period of 1955-1992. Figure 1 shows the pattern vectors for the first three components of January and July SSTs, and their corresponding coefficients are shown in Figure 2. The pattern vectors of the 2nd component represent the generally recognized El Niño-Southern Oscillation (ENSO) type of SST anomalies, whereas the first component also has a general positive area in the central and eastern tropical Pacific. The time variations of these two components, as shown by January SSTs in Figure 2, indicate that the prominent ENSO winters of 1957-1958, 1965-1966, 1972-1973, 1976-1977, 1982-1983 and 1991-1992 are characterized by the amplification of both first and second components in phase. With the July SSTs, however, it is seen that the second component of the preceding summer could indicate the onset of prominent ENSO of the following winter without the involvement of the first component. In cases of moderate to weak ENSO winters, either the first or second component is amplified, but not both of them in phase. Following this lead, the coefficients of the first and second SST components are combined in this study as their weighted mean by respective percentage variance and defined as the El Niño index (ENI). As shown in Figure 2, the ENI adequately describes various intensities of ENSO episodes documented during the period (e.g. The National Meteorological Center, 1993; World Meteorological Organization, 1987). The ENI in this study also compares favorably with Weare's (1986) ENI which was obtained in a principal component analysis over the Pacific with the dominant component in the area.
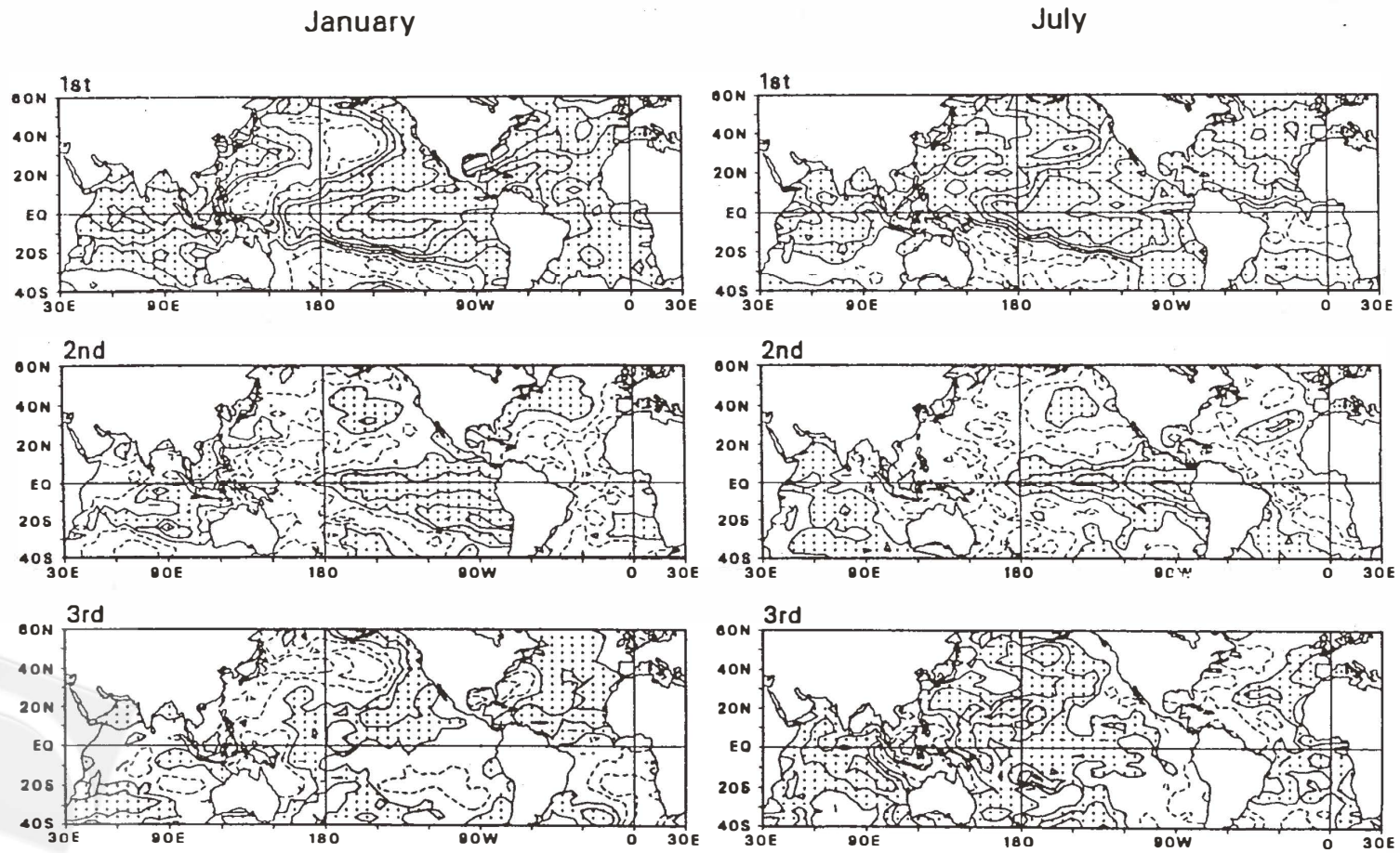
January   July

Fig. 1. Characteristic patterns (pattern vectors) for the first three principal components of January and
July SSTs during the period of 1955-1992. Positive areas are shaded. The contour interval is
0.2. (After Kung and Chern, 1994)
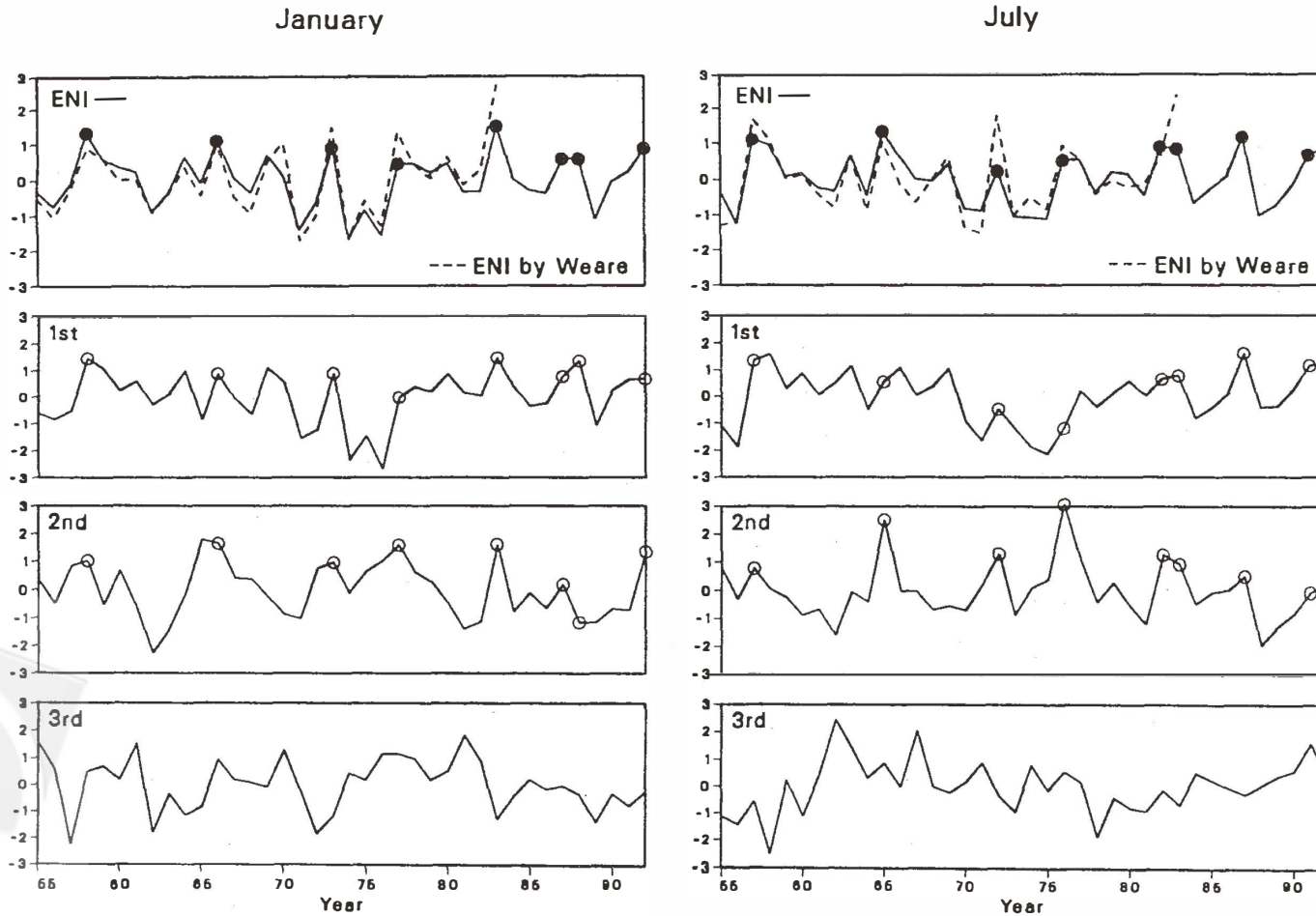
January

July

Fig. 2. Inter-annual variations of coefficients of the first three principal components of January and July SSTs during the period of 1955-1992. Dots denote years of major winter ENSO episodes. ENI is as defined in the text. ENI by Weare (1986) is represented by dashed lines. (After Kung and Chern, 1994)

In this study, the principal components of global SSTs and those of northern hemisphere geopotential height (Z) fields at 700, 500 and 300 mb levels during the period 1955-1992 are utilized to study the coupling modes of the large-scale SST and Z fields. The association of SST components and Z fields is studied on the basis of interannual variations. The utility of SST components in describing and predicting the ENSO mode of the northern hemisphere circulation is studied with the ENI as defined above. The ENSO type SSTs that have been dominant in the past decade are further analyzed with the principal components of the past few years. The predictability of local climatological variables in association with SST anomalies is studied for Taiwan Mei-Yu and for monthly temperatures and precipitation variables of climatological stations over the United States.

2. DATASETS

The output of principal component analysis of the global SSTs in a preceding study (Kung and Chern, 1994) for the period of 1955-1992 is used as direct input here wherever applicable. For the computation of separate sets of principal components for the recent data period, however, the updated monthly SST analyses for the period of 1991-1993 are the data input. For the processing of the SST dataset, reference should be made to Kung and Chern (1994).

As the output of the 1994 analysis is utilized as the data source here, some comments on the principal component analysis are pertinent. In the 1994 analysis, the anomaly fields were obtained with respect to the multi-annual means of respective monthly mean fields for the study of inter-annual variations. This eliminates the intra-annual seasonal variations. Most of the available principal component analyses of large-scale meteorological fields indicate that the first three components are sufficient to describe the large-scale variations (e.g., Kutzbach, 1967; Weare *et al.*, 1976; Park and Kung, 1988). As shown in pattern vectors of SST components (Figure 1), large-scale characteristic patterns are described mostly by the large correlation coefficients of |0.4| to |0.8|, which are significant at the 98 to 99.9% confidence level for the time period of the datasets. The higher components also show some significance in limited areas, but generally, the level of significance drops sharply. In this paper, the general discussion of the principal components is limited to the first three components. However, the higher components from the 4th to 6th are also considered in the regional discussion for Mei-Yu in Taiwan. The percentage variances of the three components as shown in Figures 1 and 2 are 17.1, 7.4 and 5.6%, respectively, for January and 12.2, 8.6 and 5.5% for July, which are compatible with previously available principal component analyses of various meteorological fields. As commented in the preceding section, it is readily seen that the pattern vectors of the 1st and 2nd components represent the generally recognized El Niño-Southern Oscillation (ENSO) type of SST anomalies.

The monthly Z fields at the 700, 500 and 300 mb levels were computed from the daily National Meteorological Center northern hemisphere octagonal grid analyses at 1500 GMT for the period of 1955-1957 and at 1200 GMT for the period of 1958-1993. The local Mei-Yu records in Taiwan for the period of 1958-1989 were provided from the archives at the Forecast Center, The Central Weather Bureau, Taiwan, R.O.C. Observations of Mei-Yu include the onset, which is expressed in terms of number of days from April 1, the Mei-Yu period in terms of days from the onset to the recess (including the onset and the recess) and total precipitation of May and June which represents the total precipitation of the Mei-Yu season. The climatological data used over the United States were obtained from the

NOAA National Climatic Data Center. This dataset consists of monthly surface temperature and precipitation records during the period of 1961-1992 at twenty four observation stations distributed throughout the country, as listed in Table 1.

Table 1. Climate stations of air temperature and precipitation records of the United States.

Station #	Station Name	Latitude (°N)	Longitude (°W)
1	Yakima, WA	46.35	-120.30
2	Casper, WY	42.51	-106.18
3	Billings, MT	45.47	-108.29
4	Reno, NV	39.32	-119.49
5	Colorado Springs, CO	38.49	-104.48
6	Salt Lake City, UT	40.45	-111.52
7	San Diego, CA	32.43	-117.10
8	Albuquerque, NM	35.05	-106.40
9	Tucson, AZ	32.15	-111.00
10	Bismarck, ND	46.48	-100.46
11	Minneapolis-St. Paul, MN	44.58	-93.15
12	Grand Rapids, MI	43.00	-85.45
13	North Platte, NE	41.08	-100.45
14	St. Louis, MO	38.39	-90.15
15	Austin, TX	30.15	-97.42
16	Little Rock, AR	34.42	-92.16
17	Syracuse, NY	43.05	-76.10
18	Burlington, VT	44.30	-73.15
19	Philadelphia, PA	40.00	-75.13
20	Roanoke, VA	37.16	-79.55
21	Cape Hatteras, NC	35.15	-75.24
22	Birmingham, AL	33.31	-86.49
23	Orlando, FL	28.32	-81.22
24	Columbia, SC	34.00	-81.00

3. ENSO MODE AND THE TROPOSPHERIC CIRCULATION

Previous works exist relating the principal components of SSTs to large-scale circulation patterns. Kawamura (1984, 1986) related the 1st and 2nd components of the North Pacific SST anomalies to the prevalent midtropospheric circulation during the northern hemisphere winter. Some seasonal dependency of atmosphere-ocean interaction over the North Pacific
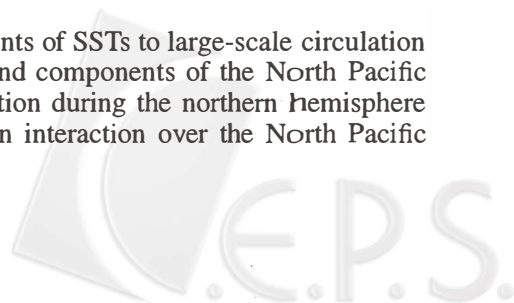
was also indicated. Kawamura's SST analysis is for the domain of the North Pacific and cannot be compared directly with the global SST analysis here, but the significant role of major SST components in forming prevailing atmospheric circulation patterns should be recognized. Yasunari's (1987) subsequent analysis of the global structure of ENSO verified the association of SST anomalies and global circulation patterns. To study the utilities of SST analysis in the long- range forecasting of the circulation with the preceding SST anomalies, unlike these previous works, the current analysis relates the major global SST components to the northern hemisphere circulation of the following seasons.

Table 2 lists the correlation coefficients between the ENIs of January, April, July and October and the first three principal components of Z fields at 700, 500 and 300 mb levels.

Table 2. Correlation coefficients of ENIs in January (a), April (b), July (c) and October (c) with the principal components of monthly Z fields at 700, 500 and 300 mb for the period of 1955-92.

(a) January ENI

Z Component		Jan.	Feb.	Mar.	Apr.	May	Jun.	Jul.	Aug.	Sep.	Oct.	Nov.	Dec.
700mb	(1st)	-.54	-.76	-.63	-.55	-.20	-.26	-.15	-.16	-.17	.05	-.20	-.20
	(2nd)	-.50	.01	-.21	-.24	.36	.21	.12	.23	.09	-.07	.10	-.02
	(3rd)	-.16	.00	-.16	.29	.17	-.28	.23	.25	.34	-.10	.01	-.31
500mb	(1st)	-.36	-.59	-.46	-.40	-.30	-.41	-.27	-.30	-.19	-.09	-.27	-.28
	(2nd)	-.44	-.08	-.19	-.32	.06	-.10	-.10	-.10	-.03	.04	.20	-.20
	(3rd)	.26	.15	-.21	-.04	.05	-.22	.11	.13	.06	-.13	.04	-.17
300mb	(1st)	-.54	-.74	-.73	-.64	-.68	-.69	-.58	-.59	-.58	-.31	-.39	-.23
	(2nd)	-.20	-.09	-.19	-.14	.25	.17	.21	.11	.09	.19	.14	.03
	(3rd)	-.17	.04	-.16	.04	.02	-.19	-.05	-.06	-.03	-.08	-.20	-.28

(b) April ENI

Z Component		Apr.	May	Jun.	Jul.	Aug.	Sep.	Oct.	Nov.	Dec.	Jan.	Feb.	Mar.
700mb	(1st)	-.54	-.22	-.39	-.27	-.27	-.24	-.04	-.14	-.34	-.04	-.03	-.07
	(2nd)	-.19	.47	.26	.18	.26	-.09	-.24	.03	-.10	-.21	.08	-.19
	(3rd)	.37	.40	-.16	.12	.42	.24	-.20	-.11	-.29	-.06	-.18	-.01
500mb	(1st)	-.44	.39	-.55	-.43	-.44	-.25	-.26	-.35	-.40	-.17	-.08	-.08
	(2nd)	-.35	.02	-.20	-.04	-.19	-.03	.00	.20	-.26	-.26	-.12	-.24
	(3rd)	.03	.16	-.14	.14	.02	.03	-.16	-.17	-.10	-.29	-.27	-.06
300mb	(1st)	-.66	-.74	-.82	-.70	-.68	-.71	-.50	-.54	-.40	-.30	-.24	-.22
	(2nd)	-.27	.14	.08	.17	-.01	-.03	.13	.19	-.04	-.22	-.02	-.16
	(3rd)	.06	.12	-.07	-.11	-.02	-.08	-.08	-.04	-.22	-.09	-.38	.31

(c) July ENI

Z Component		Jul.	Aug.	Sep.	Oct.	Nov.	Dec.	Jan.	Feb.	Mar.	Apr.	May	Jun.
700mb	(1st)	-.11	-.24	-.17	-.18	.07	-.46	-.36	-.60	-.43	-.47	-.08	-.12
	(2nd)	.33	.01	-.51	-.47	-.20	.05	-.53	-.05	-.18	-.14	.17	.07
	(3rd)	.02	.41	.01	-.42	-.33	-.07	-.06	-.08	-.14	.17	-.01	-.28
500mb	(1st)	-.18	-.17	-.09	-.26	-.22	-.46	-.37	-.57	-.43	-.45	-.33	-.32
	(2nd)	.09	-.07	-.35	.06	.03	-.08	-.54	-.08	-.16	-.13	.13	-.04
	(3rd)	.27	.01	-.11	-.41	-.39	-.09	.04	-.03	-.21	-.06	-.02	-.15
300mb	(1st)	-.38	-.25	-.33	-.41	-.39	-.51	-.55	-.74	-.67	-.62	-.57	-.51
	(2nd)	.06	-.05	-.11	-.03	.25	-.02	-.31	-.12	-.11	.05	.30	.28
	(3rd)	.21	.13	.19	-.25	.29	-.03	-.11	-.03	-.02	-.01	-.10	-.27

(d) October ENI

Z Component		Oct.	Nov.	Dec.	Jan.	Feb.	Mar.	Apr.	May	Jun.	Jul.	Aug.	Sep.
700mb	(1st)	-.07	.32	-.48	-.44	-.76	-.55	-.51	-.07	-.16	.00	.05	.03
	(2nd)	-.57	-.27	.15	-.63	-.03	-.26	-.08	.31	.28	.14	.22	.15
	(3rd)	-.42	-.30	.03	-.24	.05	-.17	.25	.02	-.27	.27	.22	.52
500mb	(1st)	-.10	-.03	-.47	-.43	-.68	-.51	-.54	-.40	-.46	-.29	-.30	-.23
	(2nd)	.06	-.12	.02	-.55	-.05	-.20	-.07	.19	.08	.08	.11	.07
	(3rd)	-.51	-.47	-.14	.09	.12	-.13	-.09	-.13	-.21	-.03	.16	.33
300mb	(1st)	-.24	-.19	-.49	-.53	-.79	-.70	-.66	-.60	-.55	-.50	-.50	-.54
	(2nd)	-.13	.26	.11	-.31	-.05	-.01	.12	.42	.35	.33	.31	.32
	(3rd)	-.29	.40	-.03	-.27	.14	-.02	-.01	-.11	-.25	-.10	-.12	-.10

(These principal components are not shown, but Figure 4 may be referred to for the general patterns of the 1st components of winter and summer circulation.) For the correlation analysis of monthly values in this study with the time period of 38 years and the degree of freedom of 36, the correlation coefficients of |0.4| to |0.8| are significant at the 98% to 99.9% confidence level. The 1st principal components at all three levels show the highest level of correlation with ENIs among the three components. With respect to the 1st Z component, the January and April ENIs show the lead time of one season in the lower troposphere and one-to-three seasons in the middle and upper troposphere. The strongest correlation is observed in February throughout all levels for the January ENI. For the April ENI, the strongest correlation appears in June at 300 mb. The July and October ENIs show a relatively low correlation with the 1st Z components for a few months, and then the ENIs tend to significantly lead the 1st Z components for the following two-to-three seasons from the lower to the upper troposphere. In particular, the 1st Z components in February show the highest correlation with the July and October ENIs. The high predictability of the winter circulation patterns with preceding summer and autumn SSTs is noteworthy.

Figure 3 illustrates the cross-correlation patterns between the July and October ENIs and the following February 700, 500 and 300 mb Z anomalies. The cross-correlation coefficients are adjusted by a minus sign, and the contour interval is 0.2. It should be noted that in the principal component analysis the sign can be reversed freely (see Preisendorfer, 1988). The cross-correlation patterns show a close resemblance to the pattern vectors of the 1st components of the February Z fields in Figure 4. It is noteworthy that these correlation patterns and pattern vectors are well defined and stable through the depth of the troposphere. This is consistent with what is shown in Table 2 where the ENI strongly influences the largest scale pattern of the tropospheric circulation at all three levels. Figure 5 shows the composite anomalies of February 700, 500 and 300 mb Z fields for the prominent ENSO episodes in 1958, 1966, 1973, 1977, 1983 and 1992. The composite anomaly patterns again show a close resemblance to the cross-correlation patterns in Figure 3 and the February pattern vectors of Z fields in Figure 4, again confirming the influence of the ENI on large scale circulation. (The pattern in Figure 4 is shown with the reverse sign.) The consistency in these patterns further verifies the utility of the ENIs of the preceding seasons to project the winter northern hemisphere circulation patterns.

Figure 6 shows the cross-correlation patterns between the ENIs of January and April with those of the following June 700, 500 and 300 mb Z anomalies. For both the January and April ENIs, similar spatial distributions of correlation are observed at all levels. The first pattern vectors of June 700, 500 and 300 mb Z are as shown in Figure 4. It is apparent again that the leading ENIs exercise a definitive control over the following summer troposphere and their effect is more clearly shown in 300 and 500 mb than in 700 mb. The intensely correlated areas are also more visible in the lower latitudes, and their strength intensifies from 700 mb to 300 mb, especially in the Pacific sector. However, the winter and spring ENIs exercise somewhat weaker direct effects on the summer circulation than do the summer and autumn ENIs on the winter circulation. The weaker effects of the leading winter and spring ENIs may be explained by the local summer forcing in the middle latitudes, whose local circulation system may act as a barrier which constrains the large-scale tropical waves to propagate to the middle latitudes (e.g., Webster, 1982). Nevertheless, the effect of the leading ENIs on the summer circulation is clear, indicating a considerable predictability of the summer circulation with the preceding SST patterns.

The essential nature of the predictability of the circulation pattern by the leading SST parameters such as the ENIs may be well related to the much longer characteristic time of
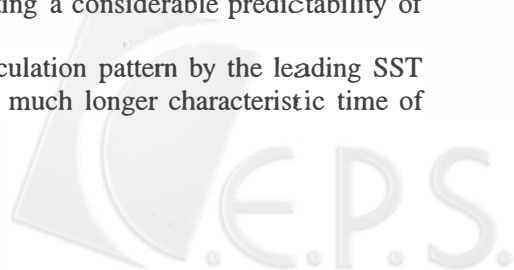
Cross-correlations of ENIs with February Upper Air Anomalies
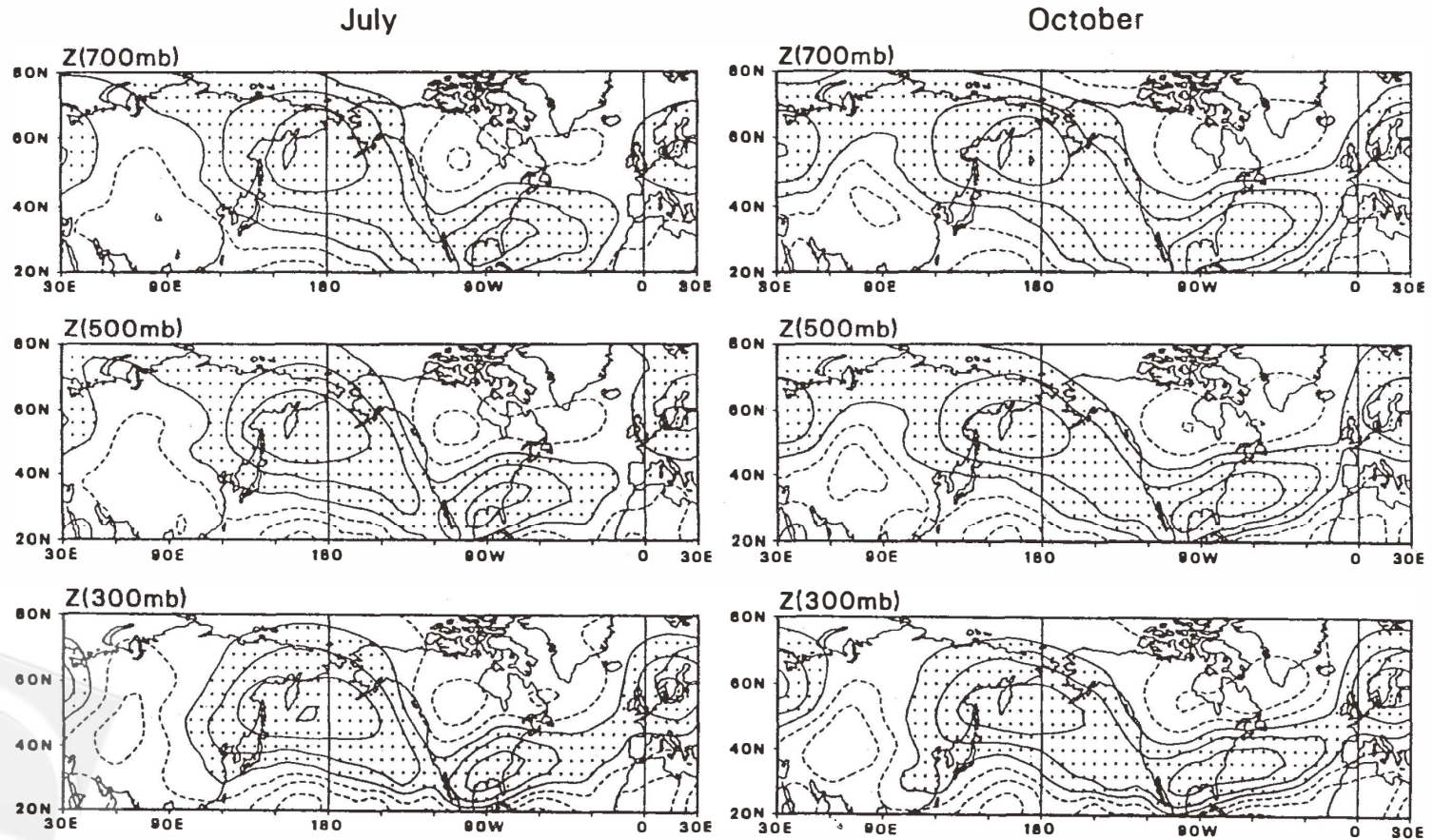
Fig. 3. Cross-correlation patterns of July and October ENIs with February Z fields at 700, 500 and 300 mb for 1958-92. Positive areas are shaded, and the contour interval is 0.2.

1st Component of Z Field
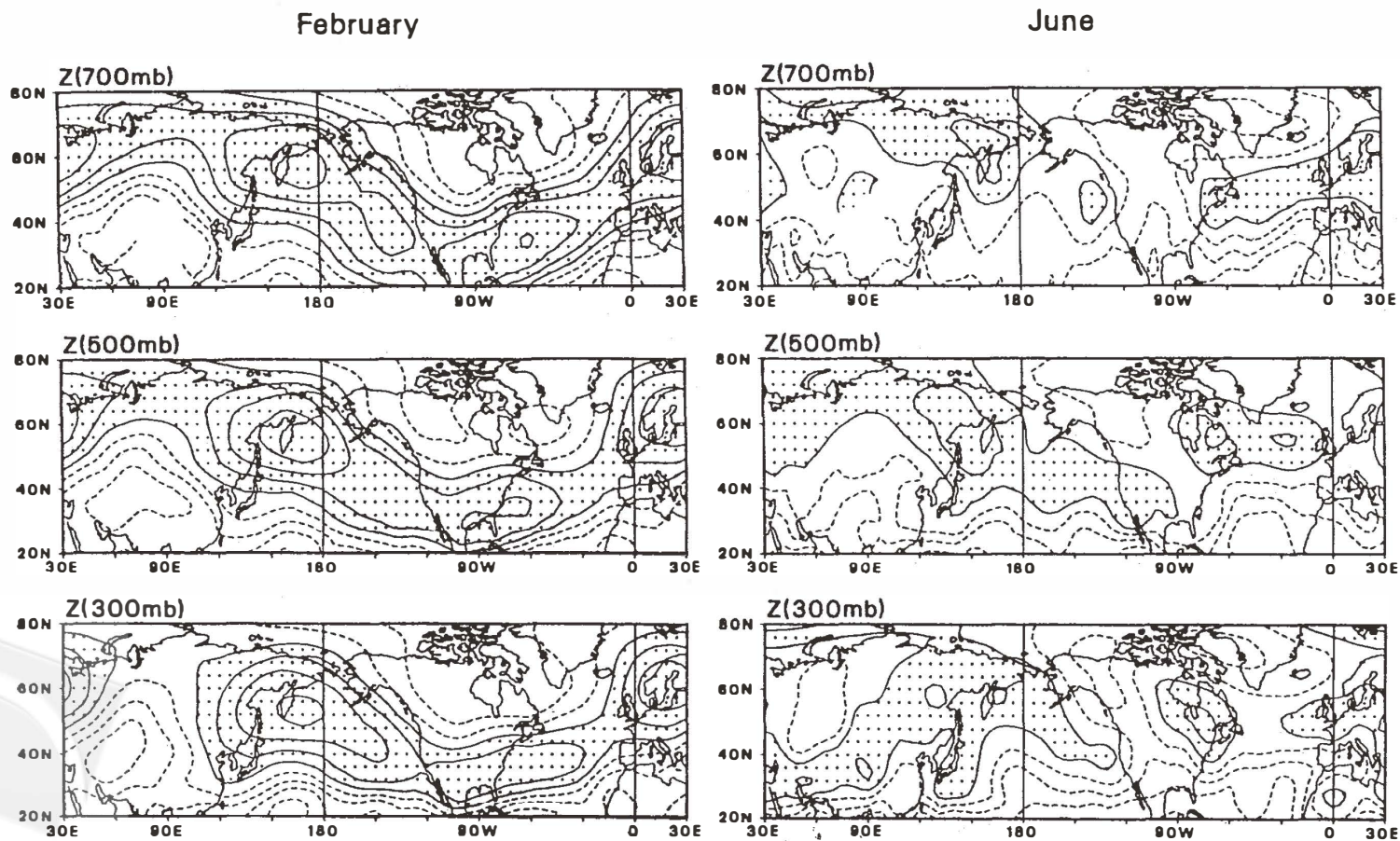
February   June

Fig. 4. Characteristic patterns of the first components of February and June Z fields at 700, 500 and 300 mb during 1955-1992. Positive areas are shaded and the contour interval is 0.2.

February ENSO Composite Flow Pattern

Z(700mb)

Z(500mb)

Z(300mb)

February ENSO Composite Anomalies

Z(700mb)

Z(500mb)
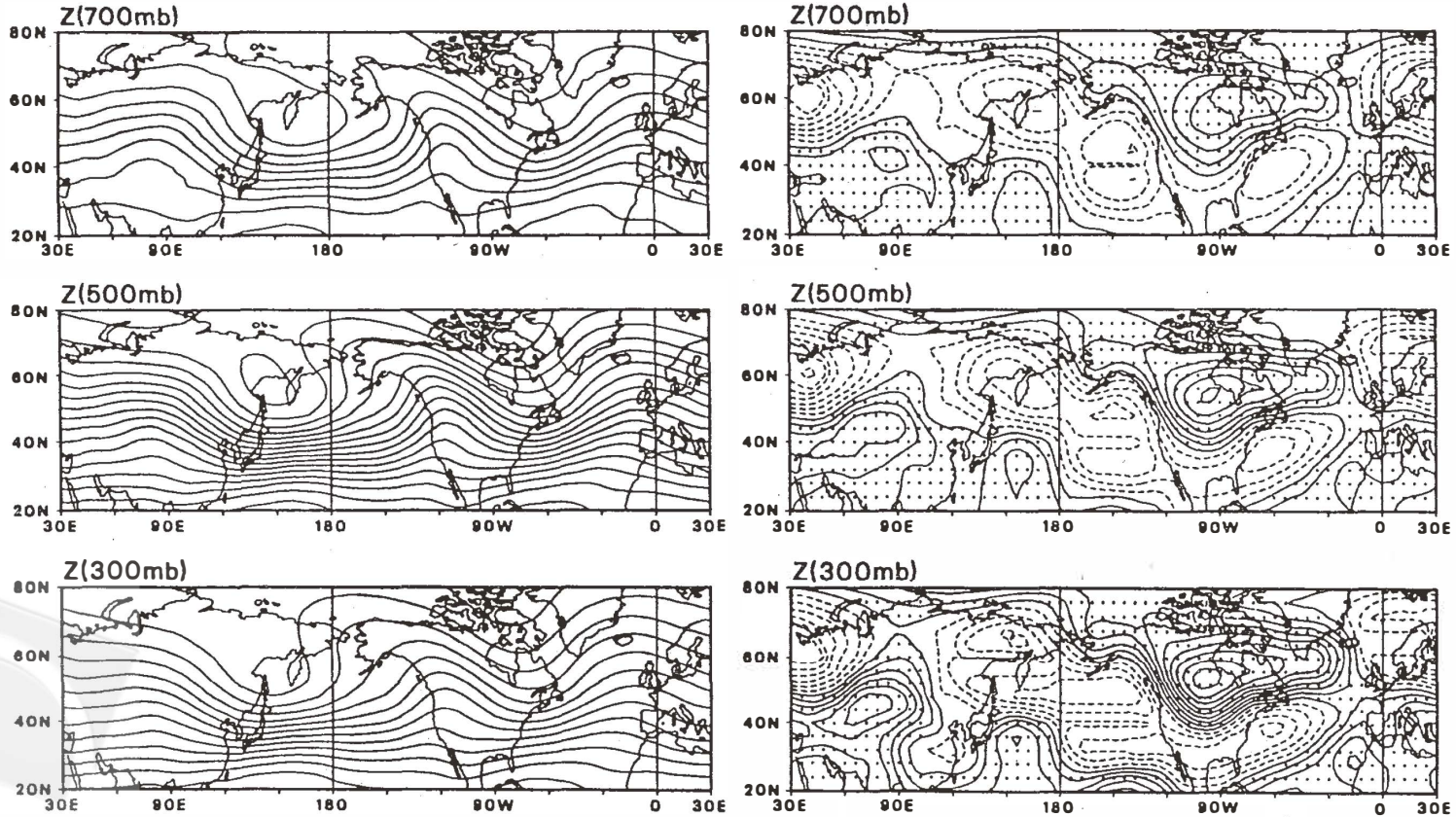
Z(300mb)

Fig. 5. Flow patterns and anomalies of February Z fields at 700, 500 and 300 mb for composites of prominent ENSO cases.

Cross-Correlations of ENIs with June Upper Air Anomalies
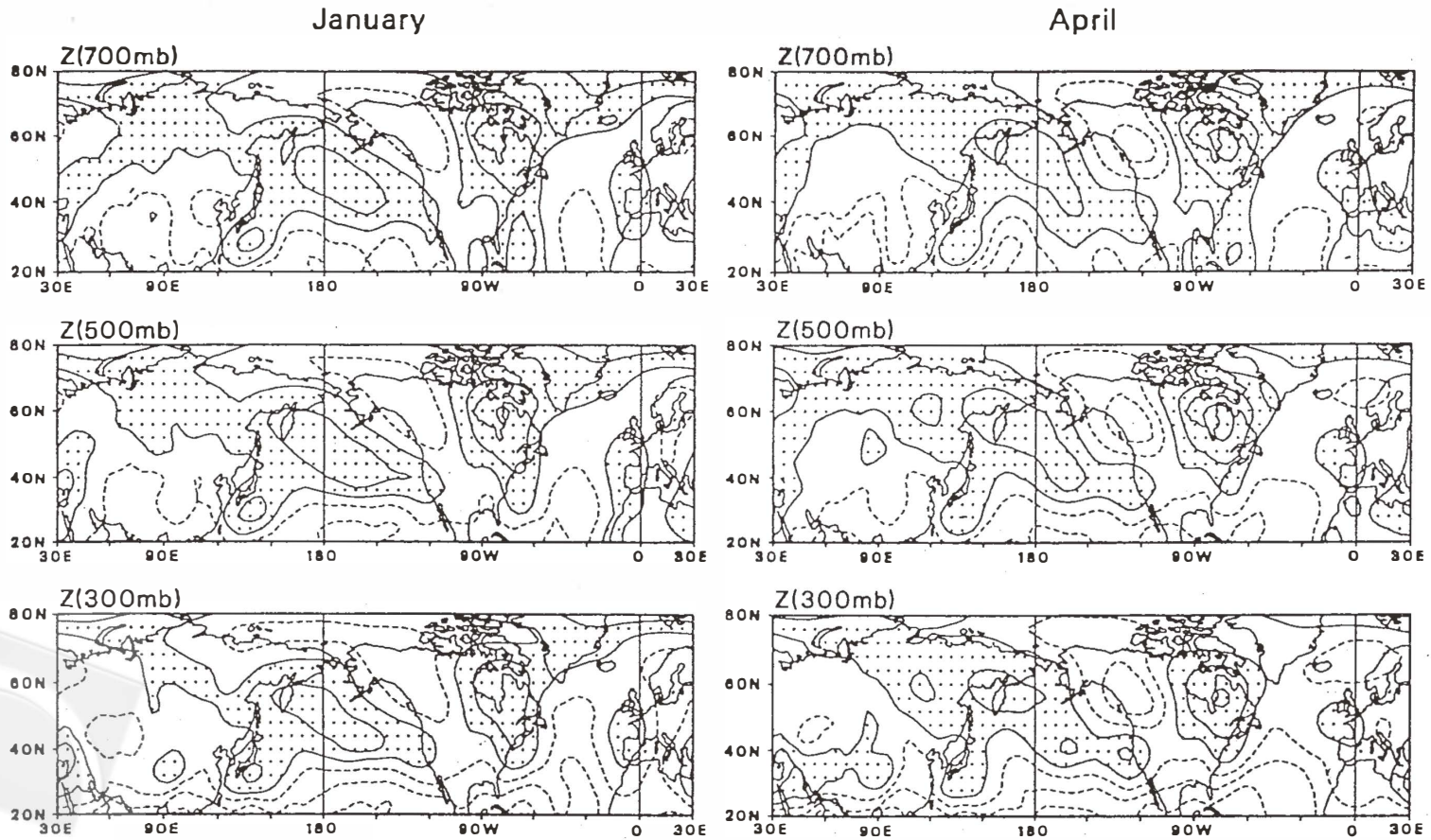
Fig. 6. Same as Figure 3, but for January and April ENIs with June Z fields.

SSTs than that of the atmospheric circulation. While slowly evolving, the persistent SST patterns for months and seasons could imply that their expected evolvement may be directly interpreted or related in terms of upper air anomalies as revealed in cross-correlation analysis.

The climate of the Northern Hemisphere over the last two decades has been characterized by recurring major ENSO events. A principal component analysis is performed for the SST data from July 1991 to December 1993. The pattern vectors are shown in Figure 7 for the 1st to 4th components. Unlike the monthly principal component analysis for 1955-1992 as presented in Figures 1 and 2, the analysis does not eliminate the intra-annual seasonal variation and uses the entire 30-month mean as the basis for calculating anomalies. The 1st component as shown in Figure 7 corresponds to the intra-annual seasonal variation as reported in Figure 4 of Kung and Chern (1994). It is noted that the positive and negative signs of pattern vectors of the principal components in Figure 7 are the reverse of those of Kung and Chern (1994). Signs of pattern vectors are given arbitrarily by the computer software and need not be of concern (see Preisendorfer, 1988).

The 2nd component in Figure 7, which is the 1st component after elimination of the seasonal variation, is comparable to the 1st component of long-term SST patterns in Figure 1. However, in the past three years, this component is much better defined than the long-term patterns in the tropics, particularly in the eastern tropical Pacific and Atlantic. In contrast, the 3rd component in the eastern tropical region is significantly weaker than the comparable 2nd component found in the long-term patterns (Figure 1). Nevertheless, a well defined subtropical to mid-latitude pattern of the southwest-northeast orientation of the 3rd component is shown in the Pacific and Atlantic north of the intensified tropical portion for the 2nd component. The 4th component is also less intense than the comparable 3rd component of the long-term patterns. The ENSO-dominated climate of the most recent three year period is associated with exceptionally strong anomalies in the tropical ocean and subtropical to mid-latitude SST patterns, respectively as shown in the 2nd and 3rd components (i.e., the 1st and 2nd component after elimination of the intra-annual seasonal component).

4. UTILITIES OF PRINCIPAL COMPONENT IN LONG-RANGE FORECASTING

In the foregoing discussions it has been shown that the major principal components of SSTs exercise controlling effects on the concurrent and following northern hemisphere circulation with a lead time of one to three seasons. In this section, Taiwan Mei-Yu and North American monthly temperature and precipitation are examined for any possible usefulness of SST components in local long-range forecasting.

4.1 Taiwan Mei-Yu

Although Mei-Yu is a local phenomenon, it is part of the global system of circulation developing in southeastern Asia parallel to the Indian summer monsoon. As described by Chen and Jou (1988), the rainfall activity during Mei-Yu in Taiwan has as its origin low-level flows, whose existence is collectively determined by the features of major circulation such as the western Pacific Subtropical High, monsoon low, major trough and mid-latitude blocking. The fact that the development of the Mei-Yu system is associated with features of global-scale circulation suggests a possible usefulness of large-scale SST variations in Mei-Yu forecasting.

Table 3 lists the 1st to 6th principal components of preceding monthly SSTs which show a significant correlation with the Mei-Yu precipitation in Taiwan at the 95% level.
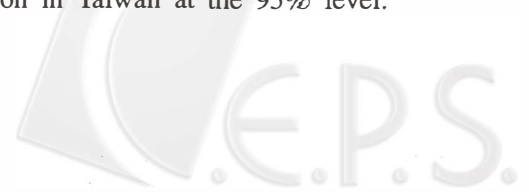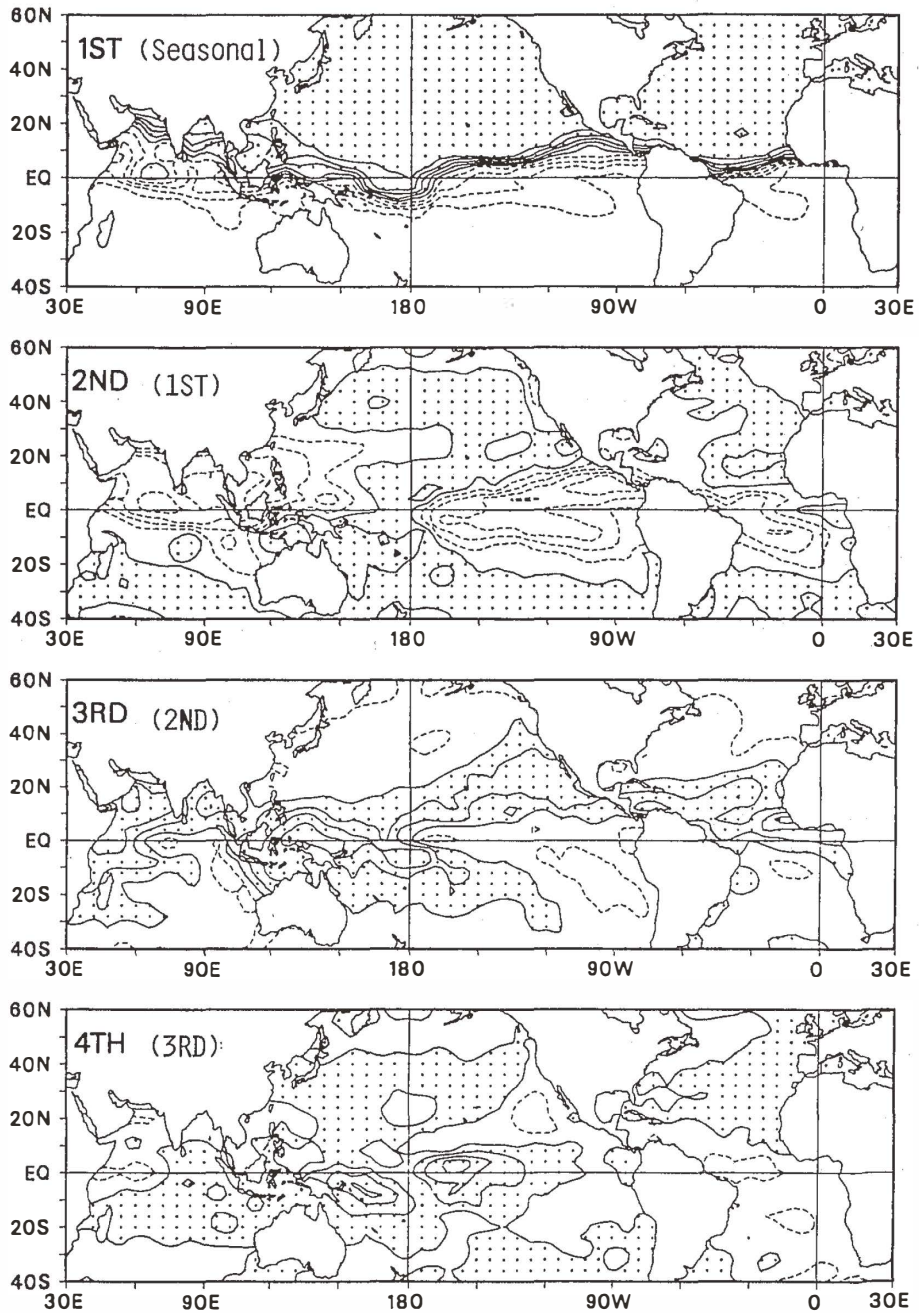
Fig. 7. Characteristic patterns for the first four principal components of monthly
SSTs for the 30-month period from July 1991 to December 1993. The
contour interval is 0.2. The identification of components in parentheses is
the order after elimination of the 1st component which is the intraannual
seasonal variation.

Table 3. Principal components of preceding monthly SSTs which show correlation at the 95% level with (a) Mei-Yu onset, (b) Mei-Yu period and (c) Mei-Yu precipitation in Taiwan. S1 is with the data of 1958-89, and S2 is with the data of 1970-89. The order of the principal components is shown between parenthesis. For instance, S2(6) means the 6th principal components of SSTs computed for the data period of 1970-89.

(a) Mei-Yu onset and preceding SST components

Oct.			Dec.			Jan.			Feb.			Mar.		
S2	(6)	.49	S1	(5)	-.44	S2	(1)	-.53	S2	(1)	.53	S2	(1)	-.47
			S2	(1)	-.48									

(b) Mei-Yu period and preceding SST components

May			Jun.			Aug.		
S1	(3)	-.36	S1	(5)	.36	S1	(6)	.36
S1	(6)	.39						

(c) Mei-Yu precipitation and preceding SST components

Jun.			Jul.			Aug.			Sep.		
S1	(1)	-.36	S1	(1)	-.41	S1	(2)	.53	S1	(2)	.49
S1	(2)	.48	S1	(2)	.48						
S2	(1)	-.48									
Oct.			Nov.			Dec.			Jan.		
S1	(2)	.40	S1	(2)	.41	S1	(2)	.40	S1	(2)	.41
						S2	(3)	-.47	S1	(5)	.39

The correlations obtained with the datasets for the period of 1958-1989 are noted by S1 and those with the 1970-1989 datasets by S2. The lag correlation in the table indicates that the Mei-Yu onset is correlated with the 1st SST components of the preceding December to March. The Mei-Yu period shows a weaker correlation, but the correlation does show a predictability of one year, if not longer. For Mei-Yu precipitation, a stable correlation with the 2nd component by S1 is identified for at least one year. The appearance of such a long predictability may be consistent with reported biennial variations of the ENSO and other circulation phenomena (e.g. Lau and Sheu, 1988; Ropelewski *et al.*, 1992).

In their multiple regression analysis, Kung and Tanaka (1985) proposed a scheme to minimize colinearity among predictors. More specifically, after determinations of the first predictor representing the largest variance, second and successive predictors are obtained by regressing the residual of fitted values and recorded climatic records on the remaining pool of possible predictors. With this approach followed, the relationship between preceding SSTs and residual components of Mei-Yu are examined. First, Mei-Yu records are fitted linearly to the preceding January ENI. The difference between the fitted and recorded Mei-Yu variable is utilized as the residual component. Figure 8 shows the result of residual analysis of the Mei-Yu onset. The correlation coefficient between the Mei-Yu onset and the January ENI is -0.55 for the 20-year period of 1970-89 which is significant at the 98% level (Figure 8a). The

residual component of the Mei-Yu onset then indicates a very strong correlation with March SST anomalies with its peak in the southwestern Pacific (16°S, 176°E) with the correlation coefficient of -0.74 which is significant at 99.9% (Figure 8b). It appears that the Mei-Yu onset can be meaningfully regressed on ENI and other small scale SST variations.

The same approach is applied to the Mei-Yu period with the result shown in Figure 9. Although the correlation coefficient is 0.26 between the Mei-Yu period and the January ENI, the residual component is well correlated with the previous October SST anomalies in the southwestern Indian Ocean (40°S, 66°E) with the large correlation coefficient of -0.77. For the Mei-Yu period, the variance from the ENI is not large, as inferred in the large correlation
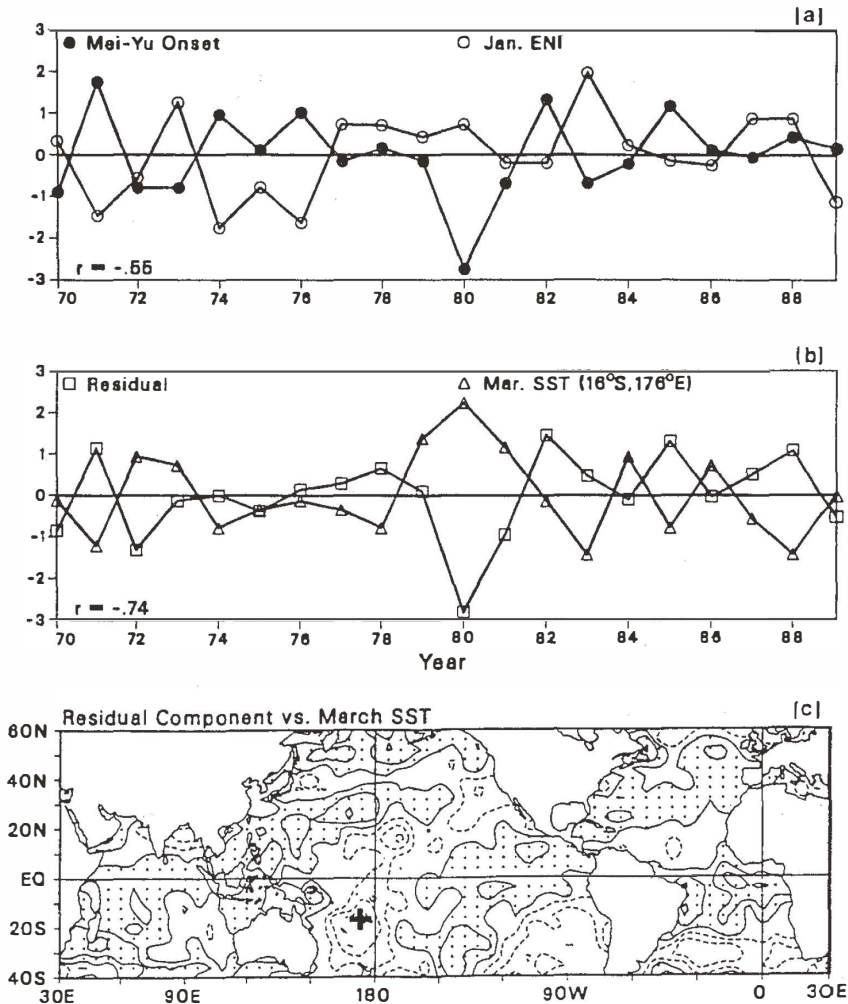
Fig. 8. (a) Normalized inter-annual variations of the Mei-Yu onset and January ENI, (b) normalized inter-annual variations of the residual component and the preceding March SST in the southeast Pacific Ocean, and (c) cross-correlation pattern of the residual component with the preceding March SST from 1970-89. Positive areas are shaded and the contour interval is 0.2.
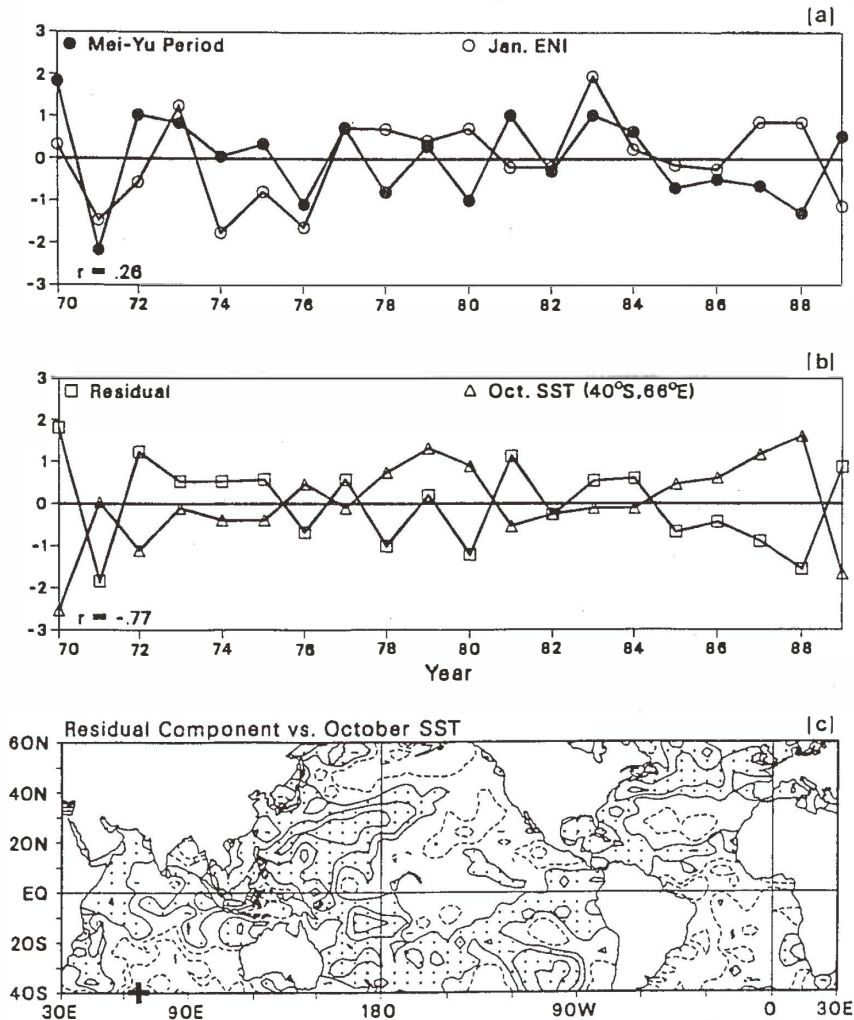
Fig. 9. Same as Figure 8, but for the Mei-Yu period.

between the residual and SST anomalies. Thus, the more localized variations seem to account for the variation of the Mei-Yu period. In both Figures 8 and 9, it is noted that the months of ENI and SST anomalies which account for the Mei-Yu variables and their residuals are not necessarily the same. This further suggests the influence of different modes of SST variation on Mei-Yu. A similar analysis for the Mei-Yu precipitation, as shown in Figure 10, indicates that the relationship between the Mei-Yu precipitation and the January ENI is nearly negligible. However, the residual component is well correlated with the preceding September SST anomalies, particularly in the Northwestern Pacific Ocean. The correlation between the residual and SST at 44°N, 156°E is -0.77.

Although phenomena during the Mei-Yu period are observed within the system of global-scale circulation, they are strongly affected by local physiographic factors in and around Taiwan. These local effects may contribute to cross-correlation patterns (Figures 8 through 10) that tend to be fragmental. In any case, the high cross-correlation of the residual
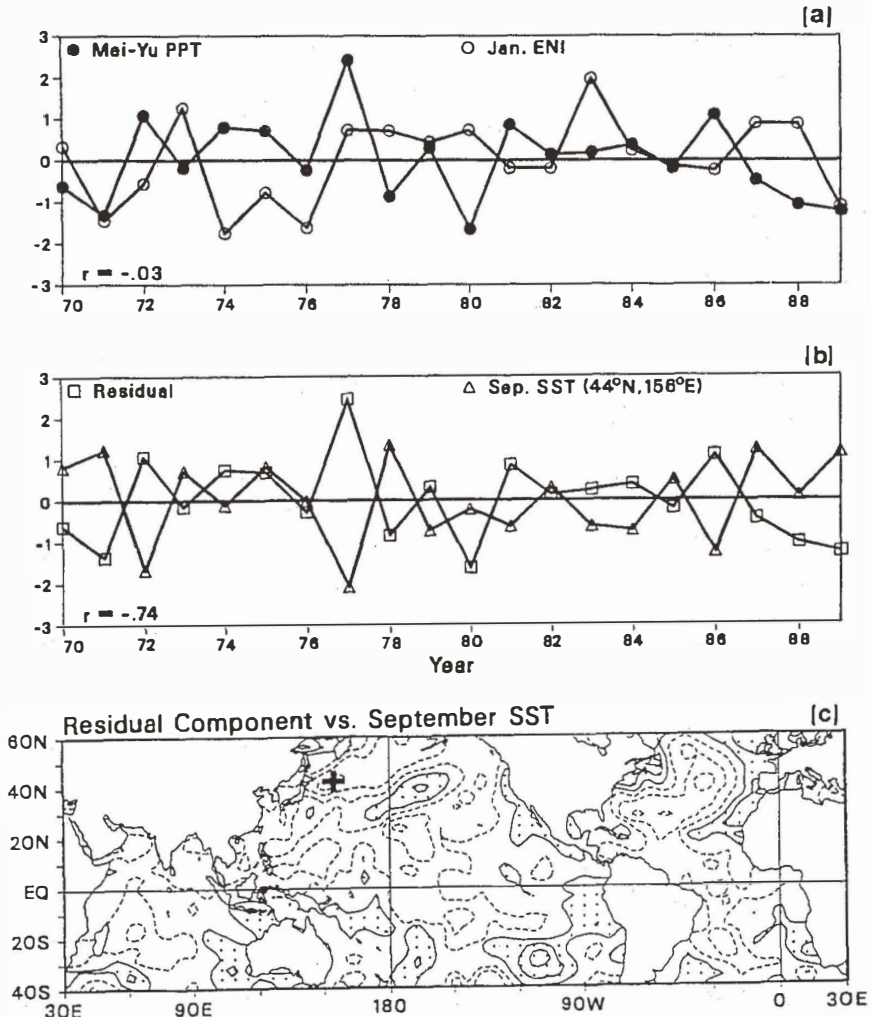
Fig. 10. Same as Figure 8, but for the Mei-Yu precipitation.

components and the preceding SST anomalies may suggest the meaningfulness of future efforts in establishing a scheme for multiple regression forecasting for the Mei-Yu events.

4.2 North American Temperature and Precipitation

Unlike Mei-Yu which is under obvious local physiographic influences, the effects of SST anomalies are readily discernable over the North American continent. In a principal component analysis of the North American summer temperature field, Park and Kung (1988) established a predictability of Midwestern summer temperature with the Pacific SST anomalies. Kung and Tanaka (1985) demonstrated the role of multiple regression in utilizing such a predictability. In that study, with climatological data from 24 observation stations over the United States (Table 1), the SST components are regarded in relation to the monthly temperatures and precipitation of these stations to examine the temporal and spacial variations of seasonal-range predictabilities of climate variables.

In this effort, the coefficients of the SST principal components for each month are correlated to the monthly temperature and precipitation records of individual stations for up to 12 months following those of SSTs. Conversely, for each month's monthly temperatures and precipitation of 24 U.S. climate stations, cross-correlations with preceding months' coefficients of SST principal components are available for up to one year. Through examination of extensive cross-correlation analysis, the 1st and 2nd SST components show meaningful correlations with temperature, but only the 1st component shows a significant relationship to precipitation. For both temperature and precipitation, stronger correlations with the SSTs of preceding seasons appear in the summer month although meaningful correlations are also observed in other seasons.

As exemplified with June temperatures in Figure 11, a noticeable predictability of June temperatures starts to appear in the preceding September for the south-central region. The pattern persists through the fall and winter and becomes less significant in spring. The pattern in the spring is not shown here, but despite the weaker pattern, the basic pattern of distribution is still observed. The weakening of signal immediately preceding the events is often observed in empirical long-range forecasting (e.g., Kung and Tanaka, 1985) and may reflect seasonal modifications from the prevailing forcing elements or delayed responses associated with nonlinear processes. As shown in Figure 12, the correlation of the 2nd SST component with June temperatures appears clearly in January in the east central and southeast regions and persists until June. The pattern is more extensive as well as stronger than that of 1st SST components. For the July precipitation, the predictability with the 1st SST component appears in September in the northeast region. As of January, the signal appears in the Great Lakes area and stays persistent until July.

The cross-correlations of SST components with regional climatic variables in the following seasons are clearly useful in the construction of an empirical regression scheme at the seasonal range. The pattern distribution as shown in Figures 11 through 13 may well represent the response of the tropospheric circulation to SST forcing in terms of wave patterns that are modified by SSTs. Thus, the correlation analysis as exemplified in this section may be utilized for the selection of SST predictors for specific regions and seasons.

5. CONCLUDING REMARKS

This paper reports one phase of the authors' continuing work in long-range forecasting. The paper describes an analytical study of the forcing SST fields and responding atmospheric circulation. No formulation of a specific forecasting scheme is involved.

The effects of SST fields are studied through the correlations of their principal components with the northern hemisphere height fields. The utility of the ENI as defined in this paper is demonstrated in predicting winter and summer circulation with the lead time of one to three seasons.

Regional forecasting of Mei-Yu involves a special difficulty in incorporating the local forcing into the large-scale forcing and responses. The residual components of SSTs as utilized in this paper might suggest a potential future approach. Regional climate variables over the United States show clear persistent responses to preceding SST components. However, a thorough teleconnections analysis is needed for the construction of a regression forecasting scheme.
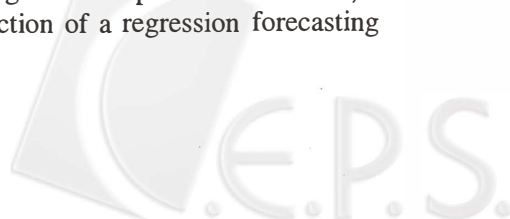
Sep SST 1st Component vs Jun Temp
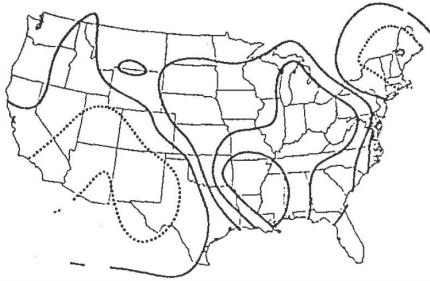
Oct SST 1st Component vs Jun Temp
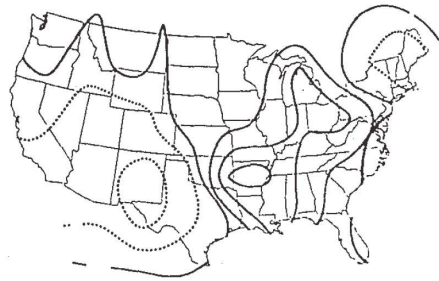
Nov SST 1st Component vs Jun Temp

Dec SST 1st Component vs Jun Temp
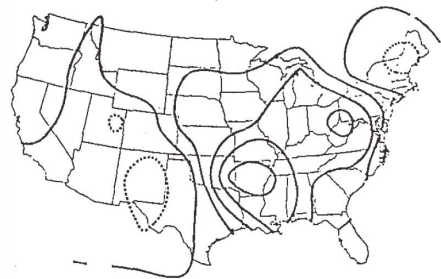
Jan SST 1st Component vs Jun Temp
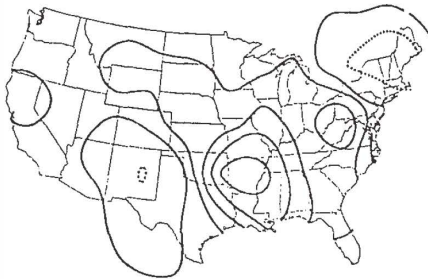
Feb SST 1st Component vs Jun Temp
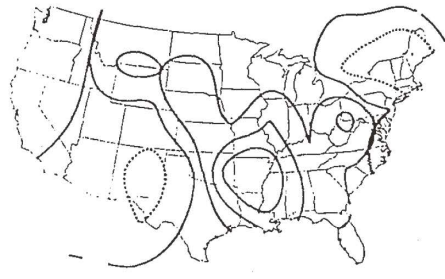
Fig. 11. Correlation patterns for the 1st principal component of SSTs with June U.S. temperatures during the period of 1961-1962. Contour interval is 0.1. The real line is for zero and positive, and the broken line for negative.

Jan SST 2nd Component vs Jun Temp
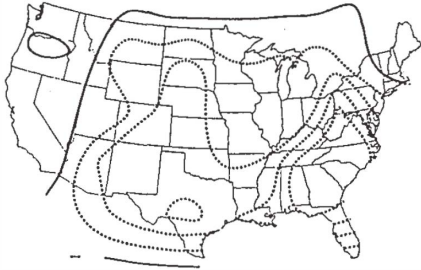
Feb SST 2nd Component vs Jun Temp
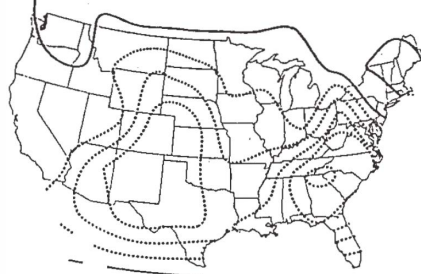
Mar SST 2nd Component vs Jun Temp
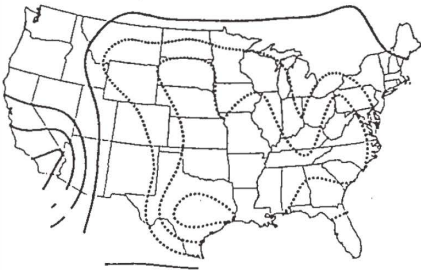
Apr SST 2nd Component vs Jun Temp
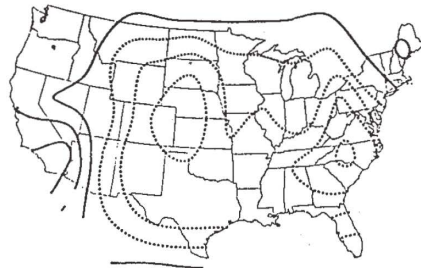
May SST 2nd Component vs Jun Temp
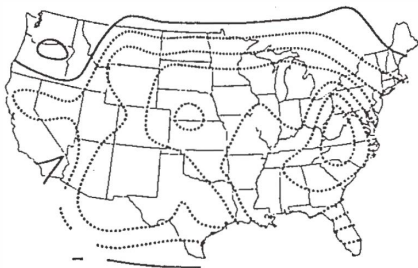
Jun SST 2nd Component vs Jun Temp
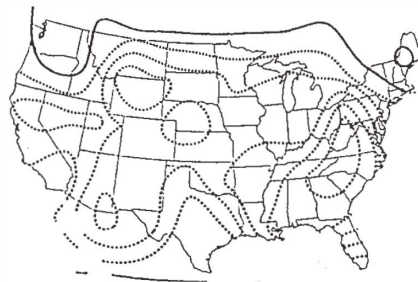
Fig. 12. Correlation patterns for the 2nd principal component of SSTs with June U.S. temperature during the period of 1961-1962. Contour interval is 0.1. The real line is for zero and positive, and the broken line for negative.

Sep SST 1st Component vs Jul Ppt

Oct SST 1st Component vs Jul Ppt

Nov SST 1st Component vs Jul Ppt

Dec SST 1st Component vs Jul Ppt

Jan SST 1st Component vs Jul Ppt

Feb SST 1st Component vs Jul Ppt
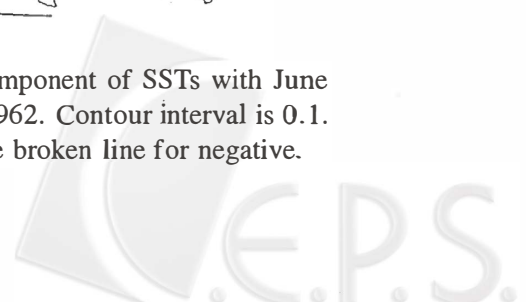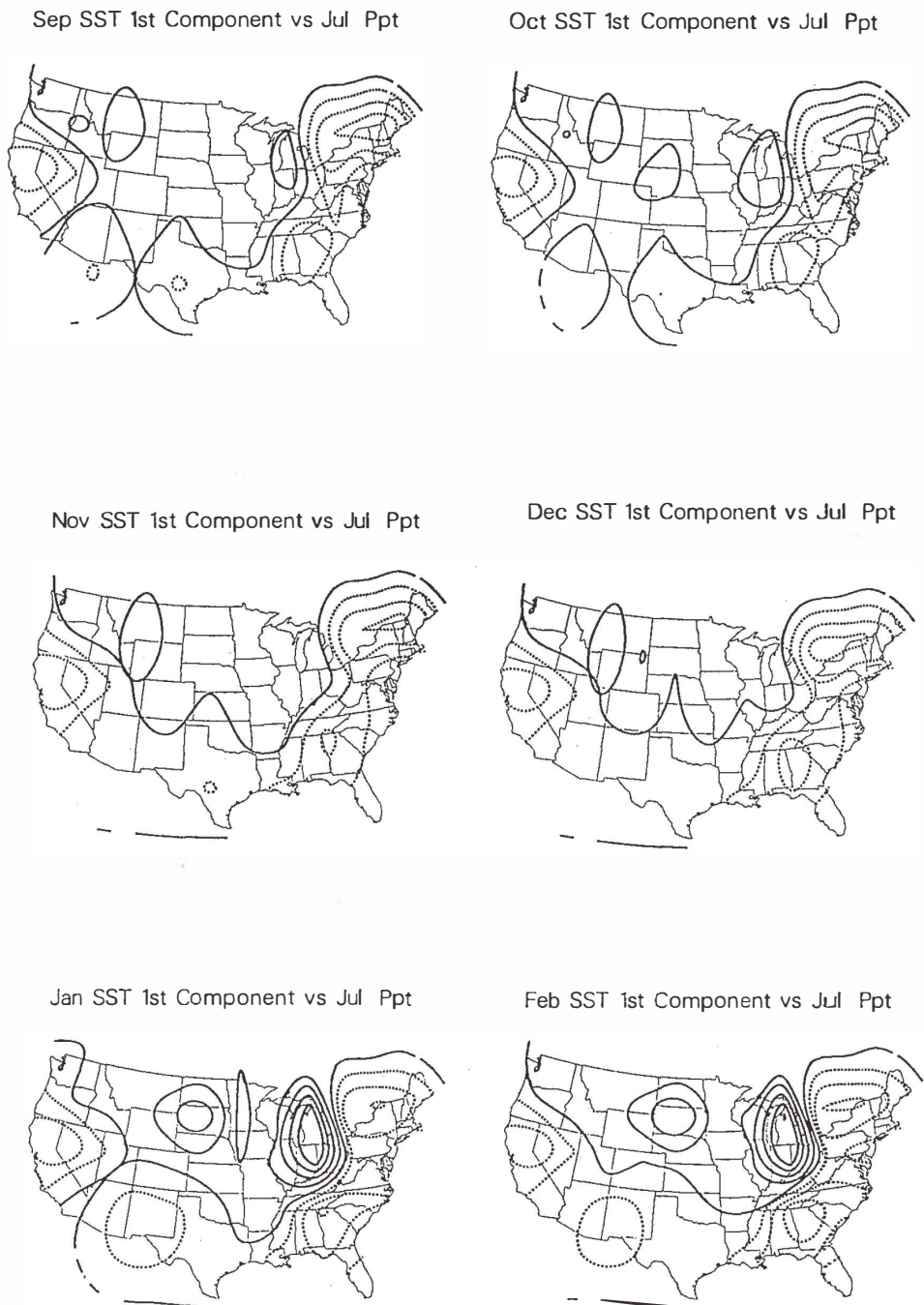
Fig. 13. Correlation pattern for the 1st principal component of SSTs and July U.S. precipitation during the period of 1961-1962. Contour interval is 0.1. The real line is for zero and positive, and the broken line for negative.

Mar SST 1st Component vs Jul Ppt
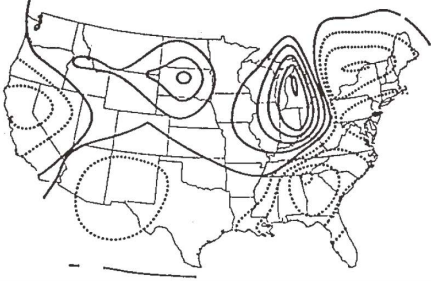
Apr SST 1st Component vs Jul Ppt
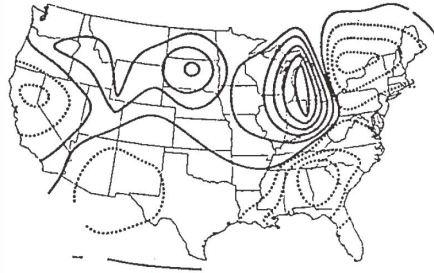
May SST 1st Component vs Jul Ppt
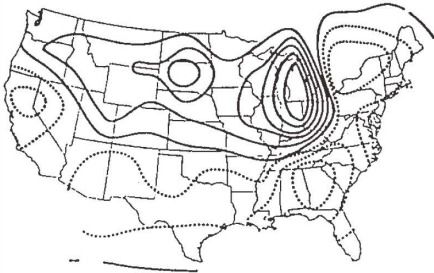
Jun SST 1st Component vs Jul Ppt
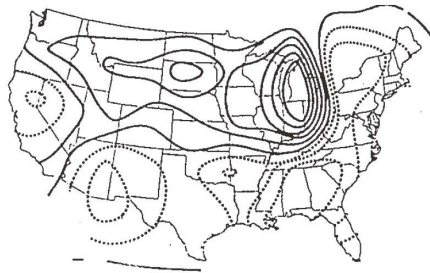
Jul SST 1st Component vs Jul Ppt
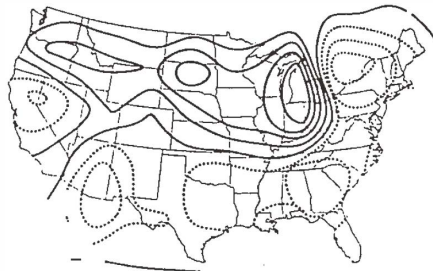
Fig. 13. (Continued.)

REFERENCES

Chen, G. T. J., and B. J. D. Jou, 1988: Interannual variations of the relevant large-scale circulations during the Taiwan Mei-Yu seasons. *Pap. Meteor. Res. Meteor. Soc. R.O.C.*, **11**, 119-147.

Heddinghaus, T. K., and E. C. Kung, 1980: An analysis of climatological patterns of the Northern Hemispheric circulation. *Mon. Wea. Rev.*, **108**, 1-17.

Kawamura, R., 1984: Relation between atmospheric circulation and dominant sea surface temperature anomaly patterns in the North Pacific during the Northern winter. *J. Meteor. Soc. Japan*, **62**, 910-916.

Kawamura, R., 1986: Seasonal dependency of atmosphere-ocean interaction over the North Pacific. *J. Meteor. Soc., Japan*, **64**, 363-371.

Kidson, J. W., 1975: Eigenvector analysis of monthly mean surface data. *Mon. Wea. Rev.*, **103**, 177-186.

Kung, E. C., and J. -G. Chern: Large-scale modes of variations in the global sea surface temperatures and Northern Hemisphere tropospheric circulation. *Atmosfera*, **7**, 143-158.

Kung, E. C., and H. Tanaka, 1985: Long-range forecasting of temperature and precipitation with upper air parameters and sea surface temperature in a multiple regression approach. *J. Meteor. Soc. Japan*, **63**, 619-631.

Kung, E. C., C. C. DaCamara, W. E. Baker, J. Susskind, and C. -K. Park, 1990: Simulations of winter blocking episodes using observed sea surface temperatures. *Quart. J. Roy. Meteor. Soc.*, **116**, 1053-1070.

Kung, E. C., W. Min, J. Susskind, and C. -K. Park, 1992: An analysis of simulated summer blocking episodes. *Quart. J. Roy. Meteor. Soc.*, **118**, 351-363.

Kutzbach, J. E., 1967: Empirical eigenvectors of sea-level pressure, surface temperature and precipitation complexes over North America. *J. Appl. Meteor.*, **6**, 761-802.

Lau, K. -M., and P. J. Sheu, 1988: Annual cycle, quasi-biennial oscillation, and Southern oscillation in global precipitation. *J. Geophys. Res.*, **93**, 10975-10988.

National Meteorological Center, 1993: Fifth Annual Climate Assessment 1993. National Weather Service NOAA. 111pp.

Park, C. -K., and E. C. Kung, 1988: Principal components of the North American summer temperature field and antecedent oceanic and atmospheric conditions. *J. Meteor. Soc. Japan*, **66**, 667-690.

Preisendorfer, R. W., 1988: Principal Component Analysis in Meteorology and Oceanography. Elsevier, 425pp.
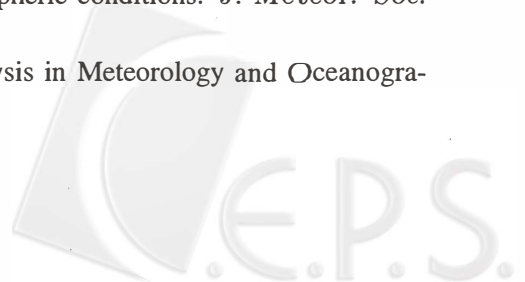
Ropelewski, C. F., and M. S. Halpert, 1992: Observed tropospheric biennial variability and its relationship to the Southern oscillation. *J. Climate*, **5**, 594-614.

Trenberth, K. E., and D. A. Paolino, 1981: Characteristic patterns of variability of sea level pressure in the Northern Hemisphere. *Mon. Wea. Rev.*, **109**, 1169-1189.

Walsh, J. E., and M. B. Richman, 1981: Seasonality in the associations between surface temperatures over the United States and the North Pacific Ocean. *Mon. Wea. Rev.*, **109**, 767-783.

Weare, B. C., 1986: An extension of an El Niño index. *Mon. Wea. Rev.*, **114**, 644-647.

Weare, B. C., A. R. Navato, and R. E. Newell, 1976: Empirical orthogonal analysis of Pacific sea surface temperature. *J. Phys. Oceanogr.*, **6**, 671-678.

Webster, P. J., 1982: Seasonality in the local and remote atmospheric response to sea surface temperature anomalies. *J. Atmos. Sci.*, **39**, 41-52.

World Meteorological Organization, 1987: The Global Climate System, CMS R84/86, 87pp.

Yasunari, T., 1987: Global structure of the El Niño/Southern Oscillation, Part I. El Niño Composites. *J. Meteor. Soc., Japan*, **65**, 67-80.